

Evaluation of the effects of irradiation on reduced-activation ferritic/martensitic steels for fusion structural materials

Sangeun Kim^{a,b}, Jinhyeok Kim^a, Kyongsik Yoo^a, Minkyu Ahn^a, Chansun Shin^a, Hyung-Ha Jin^b, Chang-Hoon Lee^c

^aDepartment of Materials Science and Engineering, Myongji University

^bNuclear Materials Safety Research Division, Korea Atomic Energy Research Institute(KAERI)

^cFerrous Alloy Department, Korea Institute of Materials Science (KIMS)

*Corresponding author: c.shin@mju.ac.kr

1. Introduction

The reduced Activation Ferritic / Martensitic (RAFM) steels are candidate materials for the blanket in a nuclear fusion reactor [1]. The composition and/or thermo-mechanical processing of RAFM steels have been modified to improve the properties of RAFM steel. It is important to evaluate the mechanical properties and environmental effects of these new alloys. Recently the mechanical properties of RAFM steels were shown to be improved by adding Ta and Ti [2]. In this study, we characterized the irradiation hardening and swelling of a newly developed Ti/Ta-RAFM steel and compared with those of Eurofer97. Irradiation hardening and swelling are characterized by using ion irradiation and He irradiation, respectively.

2. Experimental methods

The composition of Ta and Ti added RAFM steel is Fe-9wt%Cr-0.9wt%C-1wt%W-0.5wt%Ti-0.4wt%Mn-0.2wt%V-0.1wt%Ta. The steel was normalized at 1000°C for 30 minutes and tempered for 90 min at two different temperatures of 700°C and 730°C, which will be called T700 and T730, respectively hereafter.

T700, T730 and Eurofer97 (E97) samples had been irradiated by 6 MeV Fe³⁺ ions using ion accelerator in Korea Institute of Science and Technology. The irradiations have been performed in a vacuum chamber at room temperature. The total fluence was 1×10^{16} ions/cm². The depth profiles of dpa and implanted Fe-ion concentration calculated using the SRIM code [3] are presented in Fig 1(a).

200-keV He ions were implanted on the polished samples of RAFM steels using ion-beam accelerators at the Korea multi-purpose accelerator complex with a dose of 0.5×10^{17} and 1×10^{17} ions/cm² in a vacuum chamber at room temperature. A TEM grid with 50 μm opening size was attached to the surface of each polished sample before He implantation to form selective helium-implanted regions through TEM-grid holes. The depth profile of He ion distribution is displayed in Fig. 1(b) as calculated using the SRIM code.

Micro-pillars with a diameter of 500 nm were fabricated at a depth of 1.5μm from the free surface of the samples using focused ion beam milling. Non-irradiated micro-pillars were fabricated at the location

at least 30μm-away from the surface as shown in Fig. 2. The fabricated micro-pillars were compressed using nanoindenter equipped with a flat diamond tip.

The helium-implanted samples were annealed for 2 h at 300, 400, and 500°C in vacuum after detaching the TEM grid. Subsequently, the surface swelling was measured using a contactless 3D surface profiler (NV2700, NanoSystem, Korea) that has a vertical resolution of 0.1 nm using white-light scanning and phase-shift interferometry.

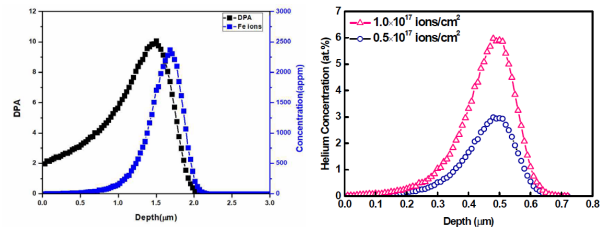


Fig. 1. (a) Depth-dependent damage and implanted ion concentration profiles and (b) depth-dependent He concentration profiles calculated using the SRIM code.

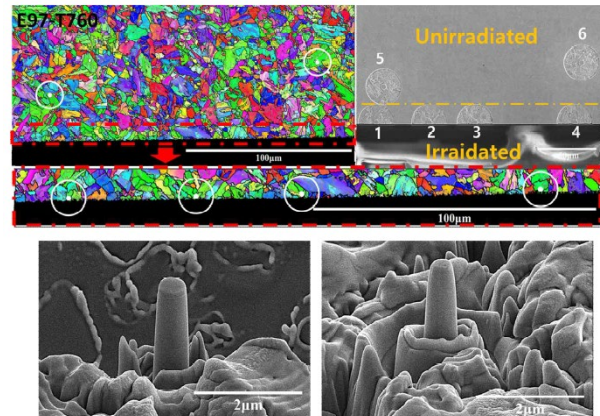


Fig. 2. EBSD map of E97, the locations of irradiated micropillars (1~4) and non-irradiated micropillars (5~6) and the SEM images of the fabricated micropillars

3. Results and discussion

The engineering stress-strain curves for non-irradiated and irradiated micro-pillars are shown in Fig. 3(a) and (b) respectively. The strengths evaluated at ~5% strain of each RAFM steels are compared in Fig. 4. The strengths of the ion irradiated micro-pillars are higher than those of the non-irradiated micro-pillars due to irradiation hardening. The change in strength due to

irradiation of Ta and Ti added RAFM steel (T700, T730) is smaller than those of E97 as shown in Fig. 4. This shows that Ta and Ti added RAFM steel is more resistant to irradiation hardening compared to E97.

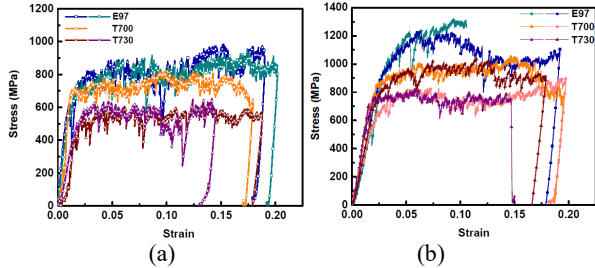


Fig. 3. The engineering stress–strain curves of (a) non-irradiated and (b) irradiated micropillars

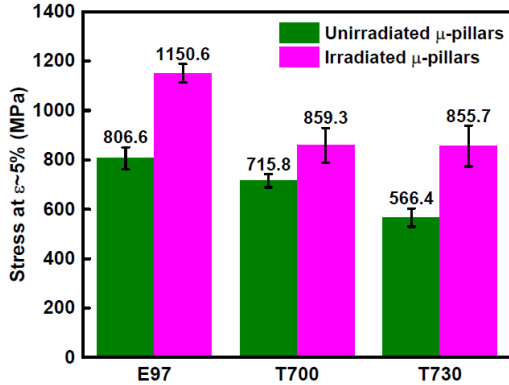


Fig. 4. Comparison of stresses at ~5% strain of each RAFM steel

Fig. 5 depicts the surface plateaus of the He-ion implanted RAFM steels measured after post-implantation annealing (PIA) by the 3D surface profiler. Aligned upheaved surface square-patterns corresponding to TEM-grid meshes are clearly visible. The step heights are measured from the surface profiles over at least 20 upheaved areas. Fig. 6 depicts the average step heights of each RAFM steel as a function of PIA temperature. First, the step height is higher for higher implanted He concentration. Second as the step height increases as PIA temperature increases. This shows that the surface swelling produced by the formation of He bubbles during PIA is more pronounced with He concentration and PIA temperatures. More interestingly the surface swelling of T730 is the smallest among the three RAFM steels. This is due to the fine distribution of MC carbides and refined $M_{23}C_6$ particles. The interfaces of between these precipitate and matrix are known to act as sink sites for He and irradiation-induced point-defects [4].

4. Conclusions

Radiation-induced hardening of newly developed Ta and Ti added RAFM steel was evaluated by self-ion irradiation and cross-sectional micropillar tests. The evaluated radiation hardening at the dose of ~10 dpa was found to be lower compared to the reference RAFM steel, Eurofer97. This represented that Ta and Ti

added RAFM steel is more resistant to irradiation hardening. The swelling of a newly developed Ti/Ta-RAFM steel was evaluated by He ion implantation at room temperature and PIA. Ta and Ti added RAFM steels tempered at 730°C showed a higher swelling resistance, and overall the swelling resistance of Ta and Ti added RAFM steels is found to be higher than that of Eurofer97.

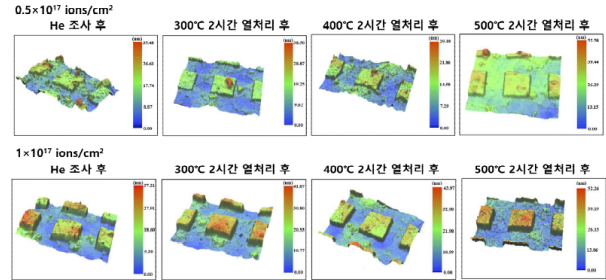


Fig. 5. Comparison of stresses at ~5% strain of each RAFM steel

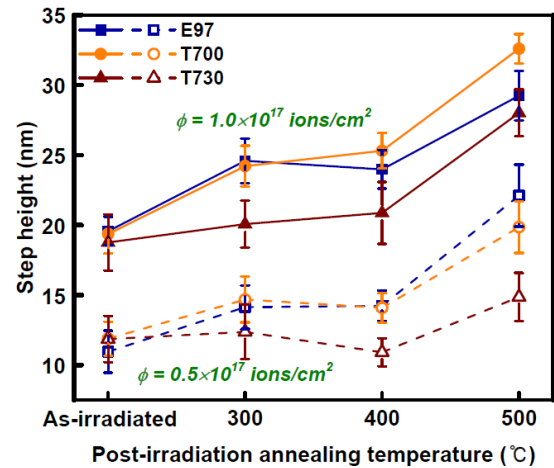


Fig. 6. Comparison of stresses at ~5% strain of each RAFM steel

REFERENCES

- [1] H. Tanigawa, E. Gaganidze, T. Hirose, M. Ando, S.J. Zinkle, R. Lindau, and E. Diegele, Development of benchmark reduced activation ferritic/martensitic steels for fusion energy applications, Nucl. Fusion 57 (2017) 092004.
- [2] H.K. Kim, J.W. Lee, J. Moon, C-H. Lee, H.U. Hong, Effects of Ti and Ta addition on microstructure stability and tensile properties of reduced activation ferritic/martensitic steel for nuclear fusion reactors, J. Nucl. Mater. 500 (2018) 327-336.
- [3] J.F. Ziegler, M.D. Ziegler, J.P. Biersack, SRIM – The stopping and range of ions in matter, Nuclear Instruments and Methods in Physics Research Section B: Beam Interactions with Materials and Atoms, Vol.268, p. 1703, 2010
- [4] Z. Jiao, N. Ham, G. S. Was, Microstructure of helium-implanted and proton-irradiated T91 ferritic/martensitic steel, Journal of Nuclear Materials, Vol 367, p. 440-445, 2007